Structural analysis of an activated sludge process with greenhouse gas emissions ⋆

Emmanuel V. B. Sampaio [*,**] **Michela Mulas** [*]
Otacílio B. L. Neto [***] **Francesco Corona** [***]

[*] *Department of Teleinformatics Engineering, Federal University of Ceará, Fortaleza, Brazil (e-mail: michela.mulas@ufc.br)*
[**] *École Centrale Nantes, Nantes, France (email: emmanuel-victor.barbosa-sampaio@eleves.ec-nantes.fr)*
[***] *School of Chemical Engineering, Aalto University, Finland, (e-mail: {otacilio.neto, francesco.corona}@aalto.fi)*

Abstract: We present a structural analysis of a class of activated sludge process models that include the dynamics and measurements describing greenhouse gas emissions. For the task, we mapped the state-space model of the process onto a complex network in which stability, controllability, and observability are studied from a structural perspective: That is, without a reference to any specific linearisation. Both weak and strong conditions are evaluated for this largely under-actuated and under-observed system with 280 state variables, 13 controls and 20 disturbances, and 33 output measurements. We show that the model is *i)* stable for almost all possible realisations of the dynamics, *ii)* full-state controllable in a weak structural sense but not in a strong sense, and *iii)* not full-state observable, for any realisation of the state-space.

Keywords: Structural control, stability, controllability, observability, activated sludge process.

1. INTRODUCTION

We are interested in the emissions of greenhouse gases (GHG), such as carbon dioxide (CO_2), nitrous oxide (N_2O), and methane (CH_4) from wastewater treatment plants (WWTPs). In WWTPs, such gases can be generated directly from the biochemical processes and indirectly from energy consumption (Huang et al., 2020). Focusing on direct emissions, long-term online monitoring of GHG from WWTPs shows that N_2O alone contributes 86% of total GHG emissions, while CH_4 and fossil CO_2 contribute 13% and about 1%, respectively (Kosonen et al., 2016).

Approaches from systems analysis based on control and optimisation are at the forefront of the technological advancements that aim at containing GHG emissions from WWTPs. Model-based approaches relying on mechanistic descriptions of wastewater treatment processes offer opportunities to understand the relationships existing between water and sludge fluxes, operational practices, as well as their connection with GHG emissions (Lu et al., 2023). In this context, Benchmark Simulation Models (BSMs), the reference platforms commonly used to describe the operation of the units in a typical WWTPs (Gernaey et al., 2014), have been widely applied for the development and verification of control-oriented strategies that address traditional WWTPs objectives. The extensions of the BSM family to include GHG emissions (from the first efforts by Flores-Alsina et al. (2011), to the recent improvements related to the dynamics of N_2O (Chen et al., 2020)) opens these models to more contemporary tasks.

⋆ This work was done for the project Control4Reuse (IC4WATER programme - Water Challenges for a Changing World, Water JPI).

In this work, we focus on the activated sludge process (ASP), as one of the main contributors of GHG in WWTPs (Huang et al., 2020). We investigate stability, controllability and observability properties of the ASP from the perspective of the biological process model by Guo and Vanrolleghem (2014). For the task, we mapped the system onto a complex network in which we studied the properties of the model from a classical and a structural point of view.

2. ASP WITH GHG EMISSIONS: PROCESS MODEL

We consider a conventional ASP for the removal of organic matter and nutrients from an influent wastewater. Specifically, we consider a process consisting of a series of five biological reactors followed by a secondary settler (Figure 1). Influent wastewater flows through the first two reactors kept in near-anoxic conditions and then through the last three rectors, which are kept in aerobic conditions by insufflating air. Wastewater from the fifth reactor is then feed to the settler, where solids are separated by sedimentation. Mixed-liquor from the fifth reactor and sludge from the settler are recirculated into the first reactor.

Nitrogen removal occurs by converting the influent ammonium (NH_4) into molecular nitrogen (N_2). This conversion is obtained by microbiological nitrification and denitrification mechanisms. The first mechanism can be described by a sequence of two aerobic reactions: the oxidation of ammonium into nitrite (NO_2) by ammonium-oxidation bacteria, and the oxidation of nitrite into nitrate (NO_3) by nitrite-oxidation bacteria. The second mechanism consists in four anoxic reactions, conducted by different heterotrophic bacteria, which reduce nitrate and nitrite into

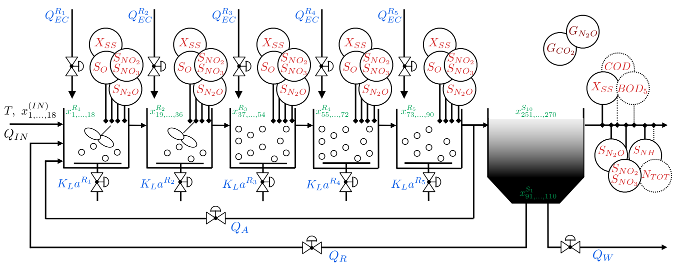

Fig. 1. The activated sludge plant.

molecular nitrogen and generate NO_2, nitric acid (NO), and nitrous oxide (N_2O) as intermediate products.

The dynamics of the five bioreactors are described by an extended Activated Sludge Model no. 1 (ASM1, Henze et al. (2006)) with *i)* a two-step nitrification and a four-step denitrification mechanism (Hiatt and Grady, 2008) and *ii)* the ASM1G addition (Guo and Vanrolleghem, 2014) to account for GHG emissions. By considering the effect of dissolved oxygen in the formation of N_2O, the ASM1G modifies the role of ammonium-oxidation bacteria in the denitrification mechanism. For the settler, the double exponential settling velocity function by Takács et al. (1991) is used for the 10-layer settling model.

Each r-th reactor ($r \in \{R_1, \dots, R_5\}$) consists of 18 state variables, $x^{(r)}$ and two controls $u^{(r)} = (K_La^{(r)}, Q_{EC}^{(r)})^T$ (the oxygen transfer coefficient and external carbon flow-rate). Each s-th layer ($s \in \{S_1, \dots, S_{10}\}$) of the settler is described by 19 state variables, $x^{(s)}$. In addition to the $u^{(r)}$, the plant is also operated through three additional controls: Internal and external recycle flow-rates (Q_A and Q_R), and wastage flow-rate Q_W. The system is subject to 20 disturbances: The influent temperature T and flow-rate Q_{IN} and its concentrations $x^{(IN)}$ entering the first reactor.

The set of state variables in the reactors and settler is

$$\begin{aligned} x^{(r)} = (&S_I^{(r)}, S_S^{(r)}, X_I^{(r)}, X_S^{(r)}, X_{BH}^{(r)}, X_{BA1}^{(r)}, X_{BA2}^{(r)}, X_P^{(r)}, \\ &S_O^{(r)}, S_{NO2}^{(r)}, S_{NO3}^{(r)}, S_{NO}^{(r)}, S_{N_2O}^{(r)}, S_{N_2}^{(r)}, S_{NH}^{(r)}, S_{ND}^{(r)}, \\ &X_{ND}^{(r)}, S_{ALK}^{(r)})^T; \\ x^{(s)} = (&S_I^{(s)}, S_S^{(s)}, X_I^{(s)}, X_S^{(s)}, X_{BH}^{(s)}, X_{BA1}^{(s)}, X_{BA2}^{(s)}, X_P^{(s)}, \\ &S_O^{(s)}, S_{NO_2}^{(s)}, S_{NO_3}^{(s)}, S_{NO}^{(s)}, S_{N_2O}^{(s)}, S_{N_2}^{(s)}, S_{NH}^{(s)}, S_{ND}^{(s)}, \\ &X_{ND}^{(s)}, S_{ALK}^{(s)}, X_{SS}^{(s)})^T. \end{aligned}$$

As for the sensors, we consider the set of measurements $y^{(r)} = (X_{SS}^{(r)}, S_O^{(r)}, S_{NO_2}^{(r)}, S_{NO_3}^{(r)}, S_{N_2O}^{(r)})^T$ from each r-th reactor, the concentrations of the effluent (from the top layer, S_{10}, of the settler) and the gas emissions in terms of carbon dioxide G_{CO_2} and nitrous oxide G_{N_2O}. Collectively,

$$\begin{aligned} y = (&y^{(R_1)}, \dots, y^{(R_5)}, S_{NO_2}^{S_{10}}, S_{NO_3}^{S_{10}}, S_{NH}^{S_{10}}, BOD_5^{S_{10}}, \\ &COD^{S_{10}}, N_{TOT}^{S_{10}}, G_{CO_2}, G_{N_2O})^T. \end{aligned}$$

According to Flores-Alsina et al. (2011), G_{CO_2} is assumed to be generated by the endogenous respiration of biomass and by nitrification and denitrification, while G_{N_2O} is only generated during nitrogen removal. As such, these concentrations can be expressed as functions of the state variables and disturbances (quality of the influent wastewater). As for the oxygen demands and total nitrogen in the effluent, usual state-output (Henze et al., 2006)) relations are used

$$\begin{aligned} BOD_5^{S_{10}} &= ((1 - f_P)((X_{BA1}^{(S_{10})} + X_{BA2}^{(S_{10})}) + \\ &\quad S_S^{(s_{10})} + X_{BH}^{(S_{10})} + X_S^{(s_{10})}))/4; \\ COD^{S_{10}} &= (S_S^{(S_{10})} + S_I^{(S_{10})}) + (X_S^{(S_{10})} + X_I^{(S_{10})} + \\ &\quad X_{BH}^{(S_{10})} + X_{BA1}^{(S_{10})} + X_{BA2}^{(S_{10})} + X_P^{(S_{10})}); \\ N_{TOT}^{S_{10}} &= (S_{NO_3}^{(S_{10})} + S_{NO}^{(S_{10})} + S_{N_2O}^{(S_{10})} + S_{NO_2}^{(S_{10})} + S_{NH}^{(S_{10})} \\ &\quad + S_{ND}^{(S_{10})} + X_{ND}^{(S_{10})}) + i_{XP}(X_P^{(S_{10})} + X_I^{(S_{10})}) \\ &\quad i_{XB}(X_{BH}^{(S_{10})} + X_{BA1}^{(S_{10})} + X_{BA2}^{(S_{10})}). \end{aligned}$$

In state-space form, the process model can be written as

$$\dot{x}(t) = f(x(t), u(t), w(t)|\theta_x); \tag{1a}$$

$$y(t) = g(x(t), w(t)|\theta_y), \tag{1b}$$

with state variables $x(t) = (x^{(R_1)}, \dots, x^{(R_5)}, x^{(S_1)}, \dots, x^{(S_{10})}) \in \mathbb{R}_{\geq 0}^{N_x}$, controls $u(t) = (u^{(R_1)}, \dots, u^{(R_5)}, Q_A, Q_R, Q_W) \in \mathbb{R}_{\geq 0}^{N_u}$, disturbances $w(t) = (T, Q_{IN}, x^{(IN)}) \in \mathbb{R}_{\geq 0}^{N_w}$, and measurements $y(t) = (y^{(R_1)}, \dots, y^{(R_5)}, S_{NO_2}^{S_{10}}, S_{NO_3}^{S_{10}}, S_{NH}^{S_{10}}, BOD_5^{S_{10}}, COD^{S_{10}}, N_{TOT}^{S_{10}}, G_{CO_2}, G_{N_2O}) \in \mathbb{R}_{\geq 0}^{N_y}$, at time t. The parameters are $\theta = (\theta_x, \theta_y) \in \mathbb{R}_{\geq 0}^{N_p}$. The model thus consists of $N_x = (18 \times 5) + (19 \times 10) = 280$ state variables, $N_u = (2 \times 5) + 3 = 13$ controls, $N_w = 2 + 18 = 20$ disturbances, and $N_y = (5 \times 5) + 8 = 33$ outputs.

3. STRUCTURAL DYNAMICS: PRELIMINARIES

The general state-space representation of a deterministic and time-homogeneous control system is given as

$$\dot{x}(t) = f(x(t), u(t), w(t)|\theta_x); \tag{2a}$$

$$y(t) = g(x(t), u(t), w(t)|\theta_y). \tag{2b}$$

The pair of functions $f(\cdot)$ and $g(\cdot)$ respectively describe how the state $x(t) \in \mathcal{X} \subseteq \mathbb{R}^{N_x}$ evolves in time and how it is emitted to form the measurements $y(t) \in \mathcal{Y} \subseteq \mathbb{R}^{N_y}$, given its value at time t and a set of controllable and non-controllable inputs $u(t) \in \mathcal{U} \subseteq \mathbb{R}^{N_u}$ and $w(t) \in \mathcal{W} \subseteq \mathbb{R}^{N_w}$. The potentially non-linear and time-varying functions are parametrised by the fixed vector $\theta = (\theta_x, \theta_y) \in \mathcal{P} \subseteq \mathbb{R}^{N_p}$.

For the structural analysis, we consider the representation

$$\dot{x}(t) = Ax(t) + Bu(t) + Ew(t) \tag{3a}$$

$$y(t) = Cx(t) + Du(t) + Fw(t) \tag{3b}$$

with matrices $A \in \mathbb{R}^{N_x \times N_x}$, $B \in \mathbb{R}^{N_x \times N_u}$, and $E \in \mathbb{R}^{N_x \times N_w}$, and $C \in \mathbb{R}^{N_y \times N_x}$, $D \in \mathbb{R}^{N_y \times N_u}$ and $F \in \mathbb{R}^{N_y \times N_w}$ are only known in a structural sense: That is, we only know whether their entries are zeros or non-zeros but potentially unknown (Reinschke, 1988). The structural system (A, B, E, C, D, F) is defined from the Jacobians of $f(\cdot)$ and $g(\cdot)$: $\partial f/\partial x$, $\partial f/\partial u$, $\partial f/\partial w$, and $\partial g/\partial x$, $\partial g/\partial u$, and $\partial g/\partial w$. Evaluating the Jacobians at specified points $(x, u, w)_{SS}$ leads to linear time-invariant approximations (LTI), with the known matrices A, B, E, C, D, and F.

3.1 *Classical properties*

For LTI systems, stability (Callier and Desoer, 1991) is a property of the system verified from the state matrix A:

Theorem 1. (Stability, LTI) Let $\Sigma(A)$ be the spectrum of A, with distinct eigenvalues $\{\lambda_i\}$ and multiplicities $\{\nu(\lambda_i)\}$

- The system is asymptotically stable IFF for any $\lambda_i \in \Sigma(A)$, we have that $\mathrm{Re}(\lambda_i) < 0$;
- The system is stable IFF for any $\lambda_i \in \Sigma(A)$, we have $\mathrm{Re}(\lambda_i) \leq 0$ and IFF for some $\lambda_i \in \Sigma(A)$ such that $\mathrm{Re}(\lambda_i) < 0$ we have that $\nu(\lambda_i) = 1$;

Similarly, controllability and observability can be verified using the usual conditions (Kalman, 1963; Hautus, 1969):

Lemma 2. (Controllability, LTI) The statement 'the pair (A, B)' is controllable is equivalent to the statements

$$\texttt{rank}(\mathcal{C}) = N_x; \tag{4a}$$

$$\texttt{det}(W_c(t)) \neq 0, \qquad \forall t > 0; \tag{4b}$$

$$\texttt{rank}([\lambda I - A\ B]) = N_x, \quad \forall \lambda \in \mathbb{C}; \tag{4c}$$

$$\texttt{rank}([\lambda_i I - A\ B]) = N_x, \quad \forall \lambda_i \in \sigma(A) \subset \mathbb{C}. \tag{4d}$$

$\mathcal{C} \in \mathbb{R}^{N_x \times N_x N_u}$ is the controllability matrix $\mathcal{C} = \begin{bmatrix} B & AB & A^2B & \cdots & A^{N_x-1}B \end{bmatrix}$, $W_c(t) \in \mathbb{R}^{N_x \times N_x}$ is the controllability Gramian $W_c(t) = \int_0^t e^{A\tau} BB^T e^{A^T\tau} \mathrm{d}\tau$.

Lemma 3. (Observability, LTI) The statement 'the pair (A, C)' is controllable is equivalent to the statements

$$\texttt{rank}(\mathcal{O}) = N_x; \tag{5a}$$

$$\texttt{det}(W_o(t)) \neq 0, \qquad \forall t > 0; \tag{5b}$$

$$\texttt{rank}(\begin{bmatrix} \lambda I - A^T & C^T \end{bmatrix}^T) = N_x, \quad \forall \lambda \in \mathbb{C}; \tag{5c}$$

$$\texttt{rank}(\begin{bmatrix} \lambda_i I - A^T & C^T \end{bmatrix}^T) = N_x, \quad \forall \lambda_i \in \sigma(A) \subset \mathbb{C}. \tag{5d}$$

$\mathcal{O} \in \mathbb{R}^{N_y N_x \times N_x}$ is the observability matrix $\mathcal{O} = \begin{bmatrix} C^T & A^TC^T & (A^T)^2C^T & \cdots & (A^T)^{N_x-1}C^T \end{bmatrix}^T$, $W_o(t) \in \mathbb{R}^{N_x \times N_x}$ is the observability Gramian $W_o(t) = \int_0^t e^{A^T\tau} C^T C e^{A\tau} \mathrm{d}\tau$.

Controllability and observability are binary properties. When verified, a number of energy-based metrics can be used to quantify control and measurement efforts from the Gramians (Pasqualetti et al., 2014). These notions were extended by Summers et al. (2016) to quantify control (measurement) efforts for single controls (sensors) directly actuating on (measuring) individual state variables.

3.2 Structural properties

System (2) can be studied from a graph of the relations between its variables. This is done by mapping the structural subsystem (A, B, C) in Eq. (3) onto the directed graph $\mathcal{G} = (\mathcal{V}, \mathcal{E})$, with vertex set $\mathcal{V} = \mathcal{V}_A \cup \mathcal{V}_B \cup \mathcal{V}_C$ (union of vertex sets $\mathcal{V}_A = \{x_1, \ldots, x_{N_x}\}$, $\mathcal{V}_B = \{u_1, \ldots, u_{N_u}\}$, $\mathcal{V}_C = \{y_1, \ldots, y_{N_y}\}$, and edge set $\mathcal{E} = \mathcal{E}_A \cup \mathcal{E}_B \cup \mathcal{E}_C$ (the union of edge sets $\mathcal{E}_A = \{(x_{n_x}, x_{n'_x}) | A_{n'_x, n_x} \neq 0\}$, $\mathcal{E}_B = \{(u_{n_u}, x_{n_x}) | B_{n_x, n_u} \neq 0\}$, $\mathcal{E}_C = \{(x_{n_x}, y_{n_y}) | C_{n_y, n_x} \neq 0\}$).

Structural stability: For a structural system (A, B, C), structural stability guarantees that if some known matrix $\bar{A}$ is stable, then all systems whose matrix A is structurally equivalent to A are also stable, for almost all possible values of its non-zero entries (Belabbas, 2013). This notion depends on the structural equivalence of two matrices.

Definition 4. (Structural equivalence, Reinschke (1988)) Matrix A and $\bar{A}$ are structurally equivalent if they have the same dimension and if each entry $A_{n'_x, n_x}$ of A is non-zero whenever the corresponding entry $\bar{A}_{n'_x, n_x}$ of $\bar{A}$ is non-zero.

Structural stability can be determined (Belabbas, 2013) from the directed subgraph $\mathcal{G}_A = (\mathcal{V}_A, \mathcal{E}_A) \subseteq \mathcal{G}$ in terms of existence of a Hamiltonian decomposition $\{\mathcal{G}_{n_g} \subset \mathcal{G}\}_{n_g=1}^{N_g}$ in disjoint subgraphs $\mathcal{G}_{n_g} = (\mathcal{V}_{n_g}, \mathcal{E}_{n_g})$, with $\cap_{n_g} \mathcal{G}_{n_g} = \emptyset$. Each subgraph $\mathcal{G}_{n_g}$ must also admit a Hamiltonian cycle. Structural stability of A is determined from the conditions:

Theorem 5. (Structural stability) Matrix A is structurally stable if it has a directed graph representation $\mathcal{G}_A$ where

- Necessary condition: $\mathcal{G}_A$ admits a Hamiltonian subgraph with n_g vertices, for each $n_g = 1, \ldots, N_x$;
- Sufficient condition: $\mathcal{G}_A$ contains the nested Hamiltonian subgraphs, $\mathcal{G}_{(1)} \subset \cdots \subset \mathcal{G}_{(n_g)} \subset \cdots \subset \mathcal{G}_A$.

Structural controllability and observability: (A, B, C) is structurally controllable (respectively, observable) if it is possible to verify the property for all possible $(\bar{A}, \bar{B}, \bar{C})$ such that (A, B) $((A, C))$ has an equivalent structure to $(\bar{A}, \bar{B})$ (respectively, $(\bar{A}, \bar{C})$) (Lin, 1974). The pairs (A, B) and $(\bar{A}, \bar{B})$ are structurally equivalent if A is structurally equivalent to $\bar{A}$ and B to $\bar{B}$. The same holds for the structural equivalence of (A, C) and $(\bar{A}, \bar{C})$. The pair (A, B) $((A, C))$ is then structurally controllable (observable) if the non-zeros of A and B (C) can be set in such a way that the resulting LTI system is controllable (observable). Formally, we have the definitions

Definition 6. (Controllability, structural) The pair (A, B) is structurally controllable IFF for some $\varepsilon > 0$, there exists a controllable pair $(\bar{A}, \bar{B})$ that is structurally equal to (A, B) and such that $||\bar{A} - A|| < \varepsilon$ and $||\bar{B} - B|| < \varepsilon$.

Definition 7. (Observability, structural) The pair (A, C) is structurally observable IFF for some $\varepsilon > 0$, there exists an observable pair $(\bar{A}, \bar{C})$ that is structurally equal to (A, C) and such that $||\bar{A} - A|| < \varepsilon$ and $||\bar{C} - C|| < \varepsilon$.

Structural controllability of (A, B) can be assessed from properties of directed subgraph $\mathcal{G}_{AB} = (\mathcal{V}_{AB}, \mathcal{E}_{AB}) \subseteq \mathcal{G}$

$$\mathcal{V}_{AB} = \mathcal{V}_A \cup \mathcal{V}_B = \{x_1, \ldots, x_{N_x}\} \cup \{u_1, \ldots, u_{N_u}\} \tag{6a}$$

$$\begin{aligned} \mathcal{E}_{AB} &= \mathcal{E}_A \cup \mathcal{E}_B \\ &= \{(x_{n_x}, x_{n'_x}) | A_{n'_x, n_x} \neq 0\} \cup \{(u_{n_u}, x_{n_x}) | B_{n_x, n_u} \neq 0\} \end{aligned} \tag{6b}$$

Theorem 8. (Controllability, structural) The pair (A, B) is said to be structurally controllable if it has a digraph representation $\mathcal{G}_{AB}$ such that the two conditions hold

- (Accessibility) For each vertex $x_{n_x} \in \mathcal{V}_A$, there exists a path from at least a vertex $u_{n_x} \in \mathcal{V}_B$ to x_{n_x};
- (Dilation-free) For all subsets $\mathcal{S} \subseteq \mathcal{V}_A$ of state vertexes, there exists a set $T_{in}(\mathcal{S}) = \{v_i \in \mathcal{V}_{AB} \mid (v_i, v_j) \in \mathcal{E}_{AB} \wedge v_j \in \mathcal{S}\}$ of $\mathcal{S}$ such that $|T_{in}(\mathcal{S})| \geq |\mathcal{S}|$.

Accessibility for $\mathcal{G}_{AB}$ can be verified with any graph search algorithm (Cormen et al. (2009)). For a graph without isolated state vertices, the dilation-free can be verified using the approach by Commault et al. (2002) based on the bipartite graph $\mathcal{K} = (\mathcal{V}^+ \cup \mathcal{V}^-, \Gamma)$, where $\mathcal{V}^+$ and $\mathcal{V}^-$ are two disjoint sets of vertices, $\mathcal{V}^+ = \{x_1^+, x_2^+, \ldots, x_{N_x}^+\} \cup \mathcal{V}_B$ and $\mathcal{V}^- = \{x_1^-, x_2^-, \ldots, x_{N_x}^-\}$. The edge set Γ of directed edges from the vertices in $\mathcal{V}^+$ to the vertices in $\mathcal{V}^-$ is defined based on $\mathcal{G}_{AB}$, in such a way that $\Gamma = \{(x_{n_x}^+, x_{n'_x}^-) | (x_{n_x}, x_{n'_x}) \in \mathcal{E}_{AB}\} \cup \{(u_{n_u}, x_{n_x}^-) | (u_{n_u}, x_{n_x}) \in \mathcal{E}_{AB}\}$. If $\mathcal{K}$ has a set of edges in which none of its elements share a common vertex, a condition denoted as matching, with a cardinality equal to N_x, then $\mathcal{G}_{AB}$ has no dilations.

Structural observability of (A, C) can be verified, by duality, from the directed graph $\mathcal{G}_{AC} = (\mathcal{V}_{AC}, \mathcal{E}_{AC}) \subseteq \mathcal{G}$,

$$\mathcal{V}_{AC} = \mathcal{V}_A \cup \mathcal{V}_C = \{x_1, \dots, x_{N_x}\} \cup \{y_1, \dots, y_{N_y}\} \tag{7a}$$
$$\mathcal{E}_{AC} = \mathcal{E}_A \cup \mathcal{E}_C \tag{7b}$$
$$= \{(x_{n_x}, x_{n'_x}) | A_{n'_x, n_x} \neq 0\} \cup \{(x_{n_x}, y_{n_y}) | C_{n_y, n_x} \neq 0\}$$

Theorem 9. (Observability, structural) The pair (A, C) is said to be structurally observable if it has a digraph representation $\mathcal{G}_{AC}$ such that the two conditions hold

- (Accessibility) For each vertex $x_{n_x} \in \mathcal{V}_A$, there exists at least one path from x_{n_x} to an vertex $y_{n_x} \in \mathcal{V}_C$
- (Contraction-free) For all subsets $\mathcal{S} \subseteq \mathcal{V}_A$ of state vertexes, there exists a set $T_{out}(\mathcal{S}) = \{v_j \in \mathcal{V}_{AC} \mid (v_i, v_j) \in \mathcal{E}_{AC} \wedge v_i \in \mathcal{S}\}$ of $\mathcal{S}$ such that $|T_{out}(\mathcal{S})| \geq |\mathcal{S}|$.

Accessibility and contraction-free for $\mathcal{G}_{AC}$ can be verified using graph search and matching algorithms (Cormen et al., 2009; Commault et al., 2002). By duality, (A, C) is observable if and only if (A^T, C^T) is controllable.

The notions and criteria of structural controllability (observability) cannot guarantee that all numerical realisations of (A, B, C) are controllable (observable) in the classical sense; There may exist numerical values of the non-zeros for which the system is not controllable (observable). Mayeda and Yamada (1979) introduced notions and criteria of strong structural controllability and observability:

Definition 10. (Strong controllability and observability, structural) For the structural system (A, B, C), we have:

- The pair (A, B) (respectively, (A, C)) is strongly controllable (observable) if any structurally equivalent realisation $(\bar{A}, \bar{B})$ of the pair (A, B) (respectively, equivalent realisation $(\bar{A}, \bar{C})$ of the pair (A, C)) is controllable (observable) in the classical sense.

Strong structural controllability (observability) of (A, B) ((A, C)), originally verified using structural and algebraic criteria (Mayeda and Yamada, 1979)-Reinschke et al. (1992), did not consider that potentially non-zeros entries of (A, B, C) may actually be zeros. Jia et al. (2020) overcomes this limitation by *i)* introducing a third type of structural entry (α) which can be either zero or non-zero, and *ii)* integrating the edge subset $\mathcal{E}_\alpha \subset \mathcal{E}$ where $\mathcal{E}_\alpha = \mathcal{E}_{A\alpha} \cup \mathcal{E}_{B\alpha} \cup \mathcal{E}_{C\alpha}$ with $\mathcal{E}_{A\alpha} = \{(x_{n_x}, x_{n'_x}) \mid A_{n_x, n_x} = \alpha\}$, $\mathcal{E}_{B\alpha} = \{(u_{n_u}, x_{n_x}) \mid B_{n_u, n_x} = \alpha\}$, and $\mathcal{E}_{C\alpha} = \{(x_{n_x}, y_{n_y}) | C_{n_x, n_y} = \alpha\}$. To determine whether (A, B) is strongly structural controllable, the conditions must hold

- Necessary condition: Matrix $M_{AB} = [A \mid B]$ is full-rank for all realisations of the pair (A, B).
- Sufficient condition: Matrix $M_{A'B} = [A' \mid B]$ is full-rank for all realisations of (A', B) with $A' \in \mathbb{R}^{N_x \times N_x}$

$$A' = \begin{cases} A'_{n_x n'_x} = A_{n_x n'_x}, & n_x \neq n'_x \\ A'_{n_x n_x} \neq 0, & A_{n_x n_x} = 0 \\ A'_{n_x n_x} = \alpha, & \text{otherwise} \end{cases}. \tag{8}$$

Strong structural controllability can then be verified using graph colouring techniques applied to the directed (sub)graphs $\mathcal{G}_{AB}$ in Eq. (6) and $\mathcal{G}_{A'B} = (\mathcal{V}_{A'B}, \mathcal{E}_{A'B})$,

$$\mathcal{V}_{A'B} = \mathcal{V}_{A'} \cup \mathcal{V}_B = \{x_1, \dots, x_{N_x}\} \cup \{u_1, \dots, u_{N_u}\} \tag{9a}$$
$$\mathcal{E}_{A'B} = \mathcal{E}_{A'} \cup \mathcal{E}_B \tag{9b}$$
$$= \{(x_{n_x}, x_{n'_x}) | A'_{n'_x, n_x} \neq 0\} \cup \{(u_{n_u}, x_{n_x}) | B_{n_x, n_u} \neq 0\}.$$

Definition 11. (Strong controllability, colouring) Consider graph $\mathcal{G}_{AB}$ (or $\mathcal{G}_{A'B}$) where all vertices are not coloured. $\mathcal{G}_{AB}$ (or $\mathcal{G}_{A'B}$) is colourable if for all state vertices

(1) We select a vertex of state x_i which is this in the neighbourhood of a vertex $v \in \mathcal{V}_{AB}$ and there exists an edge $(v, x_i) \in \mathcal{E}_{AB} - \mathcal{E}_{A\alpha} - \mathcal{E}_{B\alpha}$.
(2) x_i is coloured if it is the only uncoloured vertex in the neighbourhood of v.
(3) We repeat the process until there is no more possibility of colouring.

From Jia et al. (2020), M_{AB} is full rank for all realisations of (A, B) if $\mathcal{G}_{AB}$ is colourable and $M_{A'B}$ is full-rank for all possible realisations of the (A', B) if $\mathcal{G}_{A'B}$ is colourable.

Theorem 12. (Strong structural controllability) The pair (A, B) is strongly structurally controllable IFF

- Necessary condition: $\mathcal{G}_{AB}$ is colourable;
- Sufficient condition: $\mathcal{G}_{A'B}$ is colourable.

By duality, it is possible to check whether (A, C) is strong structurally observable from the graph representation of (A, C) and (A', C): $\mathcal{G}_{AC}$ and $\mathcal{G}_{A'C} = (\mathcal{V}_{A'C}, \mathcal{E}_{A'C})$

$$\mathcal{V}_{A'C} = \mathcal{V}_{A'} \cup \mathcal{V}_C = \{x_1, \dots, x_{N_x}\} \cup \{y_1, \dots, y_{N_y}\} \tag{10a}$$
$$\mathcal{E}_{A'C} = \mathcal{E}_{A'} \cup \mathcal{E}_C \tag{10b}$$
$$= \{(x_{n_x}, x_{n'_x}) \mid A'_{n'_x, n_x} \neq 0\} \cup \{(x_{n_x}, y_{n_y}) \mid C_{n_x, n_y} \neq 0\}$$

Both full row rank of $M_{AC} = [A|C]^T$ and $M_{A'C} = [A'|C]^T$ can be verified on $\mathcal{G}_{AC}$ and $\mathcal{G}_{A'C}$ by a colouring process:

Definition 13. (Strong observability, colouring) Consider a graph $\mathcal{G}_{AC}$ (or $\mathcal{G}_{A'C}$) where all vertices are not colored. $\mathcal{G}_{AC}$ (or $\mathcal{G}_{A'C}$) is colourable if for all state vertices

(1) We select a vertex of state x_i which is this in the neighbourhood of a vertex $v \in \mathcal{V}_{AC}$ and there exists an edge $(x_i, v) \in \mathcal{E}_{AC} - \mathcal{E}_{A\alpha} - \mathcal{E}_{C\alpha}$.
(2) x_i is coloured if it is the only uncoloured vertex in the neighbourhood of v.
(3) We repeat the process until there is no more possibility of colouring.

Theorem 14. (Strong observability, structural) The pair (A, C) is strongly structurally observable if and only if

- Necessary condition: The graph $\mathcal{G}_{AC}$ is colourable;
- Sufficient condition: The graph $\mathcal{G}_{A'C}$ is colourable.

Graph centralities: The relevance of a node in a graph is quantified by its centrality measures (Estrada and Knight, 2015). With reference to graph $\mathcal{G}_A \subset \mathcal{G}$, adjacency matrix $\widetilde{A}$ with ones wherever $\partial f / \partial x \neq 0$ and zeros elsewhere, an arbitrary vertex $x_{n_x} \in \mathcal{V}_A$, and a N_x-vector of ones (1_{N_x}),

- The in-degree $\kappa_{\text{in}}(x_{n_x}) = (\widetilde{A})_{n_x} 1_{N_x}$ is the number of edges incoming to x_{n_x}. It quantifies how pervasive are the dynamics of the other state variables are on x_{n_x};
- The out-degree $\kappa_{\text{out}}(x_{n_x}) = (\widetilde{A})^T_{n_x} 1_{N_x}$ is the number of edges departing from x_{n_x}. It quantifies how pervasive is x_{n_x} on the dynamics of other state variables.

Analogous quantities can be evaluated for the complete system graph $\mathcal{G}$, as well as for the portions $\mathcal{G}_{AB}$ and $\mathcal{G}_{AC}$. In these cases, with the additional possibility to explicitly distinguish between contributions to the in- and out-degree centralities strictly related to controls and outputs.

The in-degree is relevant for observability, as it quantifies how many state variables can be reached ('observed') by directly measuring x_{n_x}, whereas the out-degree is relevant for controllability, as it quantifies how many state variables can be reached ('controlled') by directly actuating on x_{n_x}. We refer to Bof et al. (2017) and Liu et al. (2012) for the connection between centralities and energy-based metrics.

4. ASP WITH GHG EMISSIONS: ANALYSIS

In this section, we analyse stability, full-state controllability, and observability properties of the ASP with GHG emissions (Section 2), from a structural perspective. The necessary structural representation (A, B, C) is obtained by symbolically linearising the dynamics and the measurement equation (1) to get the matrices $A = (\partial f/\partial x) \in \mathbb{R}^{280\times280}$, $B = (\partial f/\partial u) \in \mathbb{R}^{280\times13}$, and $C = (\partial g/\partial x) \in \mathbb{R}^{33\times280}$. Note that because matrices $D = (\partial g/\partial u) \in \mathbb{R}^{33\times13}$ and $F = (\partial g/\partial w) \in \mathbb{R}^{33\times20}$ are not identically equal to zero, the system's output admits a feedthrough of both controls and disturbances. The structure of the (A, B, C) portion of the state-space model is shown in Figure 2, where the associated graph $\mathcal{G} = (\mathcal{V}, \mathcal{E})$ is depicted.

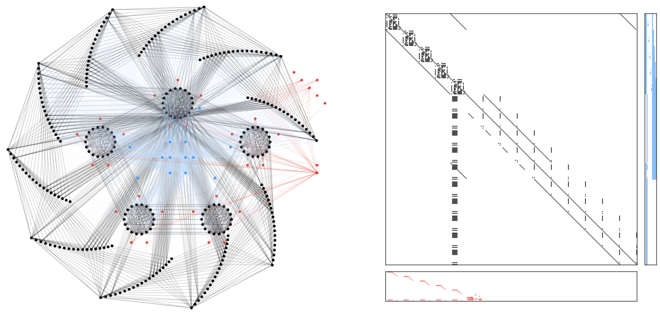

Fig. 2. Structural system (A, B, C): Left) Graph $\mathcal{G} = (\mathcal{V}, \mathcal{E})$ with state vertices in black (self-loops are omitted), control vertices in blue, and output vertices in red. Right) The structural matrices A, B, and C.

4.1 Structural properties

Stability: The stability of the model is studied from the state-state subgraph $\mathcal{G}_A \subset \mathcal{G}$ with node- and edge-set $\mathcal{V}_A = \{x_1, \ldots, x_{N_x}\}$ and $\mathcal{E}_A = \{(x_{n_x}, x_{n'_x}) | A_{n'_x,n_x} \neq 0\}$, respectively. The existence of a self-loop in each of the state variables/vertexes leads to verify the necessary and sufficient conditions for structural stability (Theorem 5), with each subgraph $\mathcal{G}_{n_g} \subset \mathcal{G}_A$ admitting a decomposition into a Hamiltonian cycle with a single vertex. Because stable in the structural sense, A is asymptotically stable almost surely (Theorem 1) also in the classical sense.

Weak controllability and observability: The controllability and observability properties of the system are firstly analysed from the input-state $\mathcal{G}_{AB} \subset \mathcal{G}$ and state-output subgraphs $\mathcal{G}_{AC} \subset \mathcal{G}$. The weak analysis is based on the verification of the conditions stated in Theorem 6 and 7. The accessibility condition in $\mathcal{G}_{AB}$ is satisfied by the existence of input vertices that reach all the state vertices. This is not true for $\mathcal{G}_{AC}$, in which a number of state-vertices (like, nitrogen gas $S^{(\cdot)}_{N_2}$ and alkalinity $S^{(\cdot)}_{ALK}$ in the reactors and the settler) cannot directly or indirectly reach any output vertex. The potential occurrence of dilations in $\mathcal{G}_{AB}$ is compensated by the existence of self-loops, which lead to a dilation-free structure, and together with its accessibility to a full-state controllable structural pair (A, B). On the other hand, the violation of the accessibility condition for $\mathcal{G}_{AC}$ leads to a pair (A, C) which is not full-state observable in a structural sense and thus in classical sense, regardless of the verification of the absence of contractions.

We conclude that for the ASP model with GHG emissions, it is possible to design a controller capable to reach any desired state in the state-space in finite time, nearly regardless of the realisation of the pair (A, B). However, it will not be possible to design an observer capable to estimate the initial state from a finite sequence of measurements, whatever the realisation of the pair (A, C): This is intuitive, when recognising the non-uniqueness of profiles in the settler that would match the measurements.

Strong controllability and observability: For all the realisations of (A, B) and (A, C) to be controllable/observable in a classical sense, the strong conditions in Theorem 12 and 14 must be satisfied. The colorability of $\mathcal{G}_{AB}$ and $\mathcal{G}_{A'B}$, and $\mathcal{G}_{AC}$ and $\mathcal{G}_{A'C}$ must be verified (Definition 11 and 13):

- $\mathcal{G}_{AB}$ is not colourable because for each node $v \in \mathcal{V}_{AB}$ (either x_{n_x} or u_{n_u}) there is more than one state vertex x_{n_x}, such that the edge (v, x_{n_x}) belongs to $\mathcal{E}_{AB}$. Pair (A, B) is controllable but not strongly controllable;
- $\mathcal{G}_{AC}$ is not colourable because the non-accessible state vertices $x_{n_x} \in \mathcal{V}_{AC}$ can not be coloured. This result reinforces what verified in terms of weak observability.

Because (A, B) is not controllable in a strong sense, there is at least one realisation of the pair that violates the conditions for classical controllability (Lemma 2). This is expected, when recognising the impossibility to enforce any arbitrary profile of soluble matter in the settler. We note that because the state matrix A is Hurwitz for almost any realisation, we can conclude that the system is still stabilisable and detectable (Callier and Desoer, 1991).

Degree centrality: The controllability results suggest that for a given controllable realisation (A, B), it is possible to design a state-feedback controller capable to control also greenhouse gas emissions $\{G_{CO_2}, G_{N_2O}\}$. These quantities are not state variables, but rather outputs depending on the state and disturbances. To quantify the magnitude of the related control efforts, we study the degree centralities of the associated state variables: The concentrations of suspended solids $\{X^{(r)}_I, X^{(r)}_S, X^{(r)}_{BH}, X^{(r)}_{BA1}, X^{(r)}_{BA2}, X^{(r)}_P\}$ and nitrous oxide $\{S^{(r)}_{N_2O}\}$ in all reactors, effluent solids $\{X^{(S_{10})}_I, X^{(S_{10})}_S, X^{(S_{10})}_{BH}, X^{(S_{10})}_{BA1}, X^{(S_{10})}_{BA2}, X^{(S_{10})}_P\}$, substrates $\{S^{(S_{10})}_S, X^{(S_{10})}_S\}$, and nitrogens $\{S^{(S_{10})}_{NH}, S^{(S_{10})}_{ND}, X^{(S_{10})}_{ND}\}$. The feedthrough controls are the aeration constants $\{K_La^{(r)}\}$, whereas the feedthrough disturbances are the influent profile $\{S^{IN}_S, X^{IN}_S, X^{IN}_{BH}, X^{IN}_{BA1}, X^{IN}_{BA2}\}$ and flow-rate Q_{IN}.

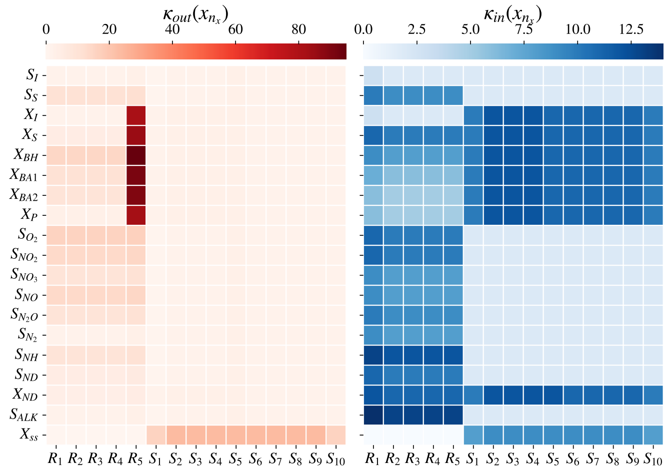

Fig. 3. Out- (left) and in-degree (right) centralities of $\mathcal{G}_A$.

The analysis of the degree centralities of $\mathcal{G}_A$ (Figure 3) shows that the out-degree of the state nodes associated with suspended solids in reactor R_5 are the largest. Therefore, the effort to control the system with only individual controls, each acting on those variables, is the smallest.

However, as those variables can only be indirectly actuated through recirculation flow-rates (Q_A and Q_R), we would need to rely on their control through directly actuating on other state-variables. This is a difficult task, as the small in-degree centralities of state-nodes associated with suspended solids (in the reactors) imply that those variables are affected by a small number of state-variables. Moreover, we note that only $\{S_O^{(r)}, S_{NO}^{(r)}, S_{N_2O}^{(r)}, S_{N_2}^{(r)}\}$ can be directly actuated through a control handle (namely, aeration $K_La^{(r)}$) in each r-th reactor. Being those variables associated with state-nodes of small out-degree centralities, we conclude that steering the process to a desired state, thus controlling the total GHG emissions, is a demanding task.

REFERENCES

Belabbas, M.A. (2013). Sparse stable systems. *Syst. Control. Lett.*, 62(10), 981–987.

Bof, N., Baggio, G., and Zampieri, S. (2017). On the role of network centrality in the controllability of complex networks. *IEEE Trans. Control. Netw.*, 4, 643–653.

Callier, F.M. and Desoer, C.A. (1991). *Linear System Theory*. Springer Texts in Electrical Engineering. Springer Science & Business Media.

Chen, H., Zeng, L., Wang, D., Zhou, Y., and Yang, X. (2020). Recent advances in nitrous oxide production and mitigation in wastewater treatment. *Water Res.*, 184, 116168.

Commault, C., Dion, J.M., van der woude, J., Van, J., and Woude, D. (2002). Characterization of generic properties of linear structured systems for efficient computations. *Kybernetika*, 38503.

Cormen, T.H., Leiserson, C.E., Rivest, R.L., and Stein, C. (2009). *Introduction to Algorithms*. MIT press.

Estrada, E. and Knight, P.A. (2015). *A First Course in Network Theory*. Oxford University Press.

Flores-Alsina, X., Corominas, L., Snip, L., and Vanrolleghem, P.A. (2011). Including greenhouse gas emissions during benchmarking of wastewater treatment plant control strategies. *Water Res.*, 45(16), 4700–4710.

Gernaey, K., Jeppsson, U., Vanrolleghem, P., and Copp, J. (eds.) (2014). *Benchmarking of Control Strategies for Wastewater Treatment Plants*. Number 23 in Scientific and Technical Report Series. IWA Publishing.

Guo, L. and Vanrolleghem, P.A. (2014). Calibration and validation of an activated sludge model for greenhouse gases no. 1 (ASMG1): prediction of temperature-dependent N2O emission dynamics. *Bioprocess Biosyst. Eng.*, 37(2), 151–163.

Hautus, M. (1969). Controllability and observability conditions of linear autonomous systems. *Indagationes Mathematicae (Proceedings)*, 72(5), 443–448.

Henze, M., Gujer, W., Mino, T., and van Loosedrecht, M. (2006). *Activated Sludge Models ASM1, ASM2, ASM2d and ASM3*. IWA Publishing.

Hiatt, W.C. and Grady, C.L. (2008). An updated process model for carbon oxidation, nitrification, and denitrification. *Water Environ. Res.*, 80(11), 2145–2156.

Huang, F., Shen, W., Zhang, X., and Seferlis, P. (2020). Impacts of dissolved oxygen control on different greenhouse gas emission sources in wastewater treatment process. *J. Clean. Prod.*, 274, 123233.

Jia, J., van Waarde, H.J., Trentelman, H.L., and Camlibel, M.K. (2020). A unifying framework for strong structural controllability. *IEEE Trans. Automat. Contr.*, 66(1), 391–398.

Kalman, R. (1963). Mathematical description of linear dynamical systems. *Journal of The Society for Industrial and Applied Mathematics, Series A: Control*, 1, 152–192.

Kosonen, H., Heinonen, M., Mikola, A., Haimi, H., Mulas, M., Corona, F., and Vahala, R. (2016). Nitrous oxide production at a fully covered wastewater treatment plant: Results of a long-term online monitoring campaign. *Environ. Sci. Technol.*, 50(11), 5547–5554.

Lin, C.T. (1974). Structural controllability. *IEEE Trans. Automat. Contr.*, 19(3), 201–208.

Liu, Y.Y., Slotine, J.J., and Barabasi, A.L. (2012). Control centrality and hierarchical structure in complex networks. *PLOS ONE*, 7(9), 1–7.

Lu, H., Wang, H., Wu, Q., Luo, H., Zhao, Q., Liu, B., Si, Q., Zheng, S., Guo, W., and Ren, N. (2023). Automatic control and optimal operation for greenhouse gas mitigation in sustainable wastewater treatment plants: A review. *Sci. Total Environ.*, 855, 158849.

Mayeda, H. and Yamada, T. (1979). Strong structural controllability. *SIAM J Control Optim.*, 17(1), 123–138.

Pasqualetti, F., Zampieri, S., and Bullo, F. (2014). Controllability metrics, limitations and algorithms for complex networks. *IEEE Trans. Control. Netw.*, 1(1), 40–52.

Reinschke, K., Svaricek, F., and Wend, H.D. (1992). On strong structural controllability of linear systems. In *[1992] Proceedings of the 31st IEEE Conference on Decision and Control*, 203–208. IEEE.

Reinschke, K.J. (1988). *Multivariable Control: a Graph-theoretic Approach*. Springer.

Summers, T.H., Cortesi, F.L., and Lygeros, J. (2016). On submodularity and controllability in complex dynamical networks. *IEEE Trans. Control. Netw.*, 3(1), 91–101.

Takács, I., Patry, G.G., and Nolasco, D. (1991). A dynamic model of the clarification-thickening process. *Water Res.*, 25(10), 1263–1271.